Journal of Indian Acad. Math. ISSN: 0970-5120
Vol. 47, No. 1 (2025) pp. 231-249

*Hemangini Shukla*[1]
*Shivanshi Dave*[2]
*Kapil K Dave*[3]
*A. K. Rathod*[4]
*N. D. Patel*[5]
*and*
*J. A. Prajapati*[6]

# INVARIANT ANALYSIS OF HEAT GENERATION AND THERMAL RADIATION EFFECTS ON MHD NON-NEWTONIAN POWER-LAW NANOFLUID OVER LINEARLY STRETCHING SURFACE WITH CONVECTIVE BOUNDARY CONDITIONS

**Abstract:** This study examines the effects of thermal radiation and heat generation along a stretching surface. The power-law non-Newtonian model under the influence of Brownian motion and thermophoresis for nanofluids is analysed for determining their effects on various parameters of nanofluid like temperature, velocity etc. The uniform magnetic field and boundary conditions for convective mode are also considered for nanofluid flow. The objective of similarity invariants is to convert non-linear partial differential equations into ordinary differential equations invariantly. The numerical results of the investigation for the impacts of various parameters on skin friction coefficients, Nusselt-Sherwood numbers are determined. The behaviour of different physical factors on skin friction coefficients in $x$ and $y$ directions, on the local Nusselt number, and on the Sherwood number is analysed. An increment in the power-law index increases the Nusselt number. The results of the experiment indicates that an increase in the heat generation parameter will result in a drop in the Nusselt number and an increase in the Sherwood number. Sherwood number will decrease and Nusselt number will increase with an increase in thermal radiation parameter.

**Keywords:** MHD Nanofluid; Non-Newtonian Power-law Model; Heat Generation and Radiation; Similarity Invariants; Convective Boundary Condition.

**Mathematics Subject Classification No.:** 35Q35, 76M60, 58J70, 35G60.

## 1. Introduction

The dispersion of nanoparticles in a base fluid, such as water, ethylene glycol, or oil, is known as nanofluid. It was introduced and studied by Choi(1995). In his experimental research, he also noticed that heat transfer was enhanced in nanofluid compared to regular fluids. There are many attractive applications of nanofluid like coolants, brake fluid, gear lubrication in automobile industries. It is useful in solar devices, as delivery of cancer drugs in the medical field, and coolants in electronic devices. So, it is an essential to study the influence of different physical factors and various physical situations on nanofluid flow.

Tesfaye *et al*. (2020) analysed the erratic flow of Williamson nanofluid over a stretched sheet under the influence of a magnetic field, heat radiation, and chemical reaction. Kalidas *et al*. (2018) examined heat generation/absorption effects for Oldroyd-B type nanofluid, two-dimensional flow over a permeable stretching surface under the effect of magnetic field and slip velocity. Umadevi and Nithyadevi (2016) investigated two-dimensional nanofluid flows under uniform heat generation or absorption with a uniform magnetic field for different thermal boundaries. Bilal *et al*. (2018) examined the impact of the various physical factors for three-dimensional Maxwell nanofluid MHD flow passing through a bidirectional stretching surface under nonlinear thermal radiation. Hayat *et al*. (2017) addressed three-dimensional Maxwell MHD nanofluid flow under the influence of heat generation-absorption and thermal radiation on a stretching surface. Burger's nano-liquid flow over a stretching sheet was studied by Ganesh *et al*. (2018) with the impact of non-linear radiation and non-uniform heat generation and absorption. The thermal radiation effects on the MHD stagnation point, the two-dimensional flow of a non-Newtonian Williamson fluid, over a stretching plate, were examined by Hasmawani *et al*. (2019) by applying similarity transformations. The two-dimensional flow of Maxwell nanofluid on a linearly stretching surface under heat generation and absorption impacts was investigated by Awais *et al*. (2015). The two-dimensional flow passing over an exponentially stretching sheet of MHD Casson fluid was studied with internal heat generation by Animasaun *et al*. (2016).

Waqas *et al*. (2017) modelled and analysed Oldroyd-B nano-liquid two-dimensional flow over a moving sheet with heat generation and absorption effects using the Homotopy analysis method. The MHD nanofluid three- dimensional flow over a shrinking sheet under viscous dissipation and heat generation and absorption with entropy generation was examined by Hiranmoy *et al*. (2019). The solution for unsteady, two-dimensional nanofluid flow over a stretching surface was studied numerically by utilising the fourth-fifth order RKF technique under the influence of radiation, thermophoresis, and heat generation and absorption by Pandey and Manoj (2018). Ahmed *et al*. (2019) examined MHD Maxwell nanofluids flow over a

stretching surface under the influence of heat generation-absorption and non-linear thermal radiation in the porous medium by applying similarity variables and the shooting technique. Kalpna and Sumit (2017) investigated two- dimensional (MHD) Jeffrey nanofluid flow in the presence of thermal radiation, heat generation/absorption, and viscous dissipation over an impermeable surface by assuming similarity transformations and applying the Homotopy analysis method. Makinde (2011) introduced similarity variables and used the fourth-order Runge-Kutta method and the shooting method to examine the impacts of internal heat generation on two-dimensional boundary layer flow on a vertical plate with a convective surface boundary condition. Lalrinpuia and Surender (2019) used the homotopy analysis approach to assess MHD nanofluid flow in a saturated porous medium, in an inclined channel with a heat source/sink, accounting for hydrodynamic slip and convection at the boundary. Khan et al. (2014) analysed the impacts of heat generation/ absorption on the 3-D flow of an Oldroyd-B nanofluid over a sheet stretching in both x and y directions. They applied similarity transformations.

The influence of heat generation, radiation, and viscous dissipation on the flow of MHD nanofluid over a sheet stretched exponentially in a porous medium was studied by Thiagarajan and Dinesh Kumar (2019). The MHD-Carreau nanofluid flow over a radially stretched sheet under the influence of chemical reaction, nonlinear thermal radiation, and heat generation/absorption was examined by Dianchen *et al*. (2018). The second grade Cattaneo-Christov two-dimensional fluid flow caused by a linear stretched Riga plate was studied under the impact of heat generation/absorption by Aisha *et al*. (2018). Abdul Khan *et al*. (2018) analysed Williamson nanofluid flow in three dimensions across a linear porous stretching surface for the impact of thermal radiation. Sulochana *et al*. (2016) investigated Newtonian and non-Newtonian, 3-D magnetohydrodynamic fluid flow across a stretched sheet. Chuo-Jeng and Kuo-Ann (2021) examined the effects of zero nanoparticle flux, internal heat generation, nonlinear radiation, and changing viscosity on free convection on a non-Newtonian power-law nanofluid flowing via a vertical truncated cone embedded in a fluid-saturated porous medium. Considering thermal radiation and heat absorption/generation, Mabood *et al*. (2020) investigated MHD Oldroyd-B two-dimensional, thermal stratified flow across an inclined linearly stretched sheet. Recently, Newtonian and various non-Newtonian fluid models like Sisko, Powell-Eyring, Power-Law Model, Prandtl-Eyring were analysed using invariant analysis via the group- theoretic technique by deriving dependent and independent invariants. (Patel *et al*. 2015, Shukla *et al*. 2017, 2018, 2020). Impact of heat generation/absorption in the context of nonlinear thermal radiation on magnetohydrodynamic stagnation-point two-dimensional Newtonian nanofluid flow across a convective stretching surface were examined by Feroz *et al*. (2018). Shukla *et al*. (2020) analysed flow over linearly stretching surface for 3-D Power-low nanofluid.

Due to the significance role of heat generation and thermal radiation on nanofluid flow, we have extended the work done by Shukla *et al*. (2020) and considered the influence of heat generation and thermal radiation. In this paper, we have studied a power-law fluid flow in three dimensions on a linearly stretched sheet. A survey of the literature shows that most studies have focused on flows in two directions, X and Y. The scenario is more real in three dimensions, X, Y, and Z. We have also examined the effects of thermophoresis, magnetic field, and Brownian motion on heat generation and thermal radiation. The convective boundary conditions have been considered for the analysis of the present non-Newtonian fluid flow model. Various parameters like Nusselt number, skin friction coefficients, and Sherwood number have been considered for analysing the flow. Similarity-dependent and independent invariants have been used with the aim of transforming the nonlinear PDEs into ODEs invariantly.

## 2. Governing Equation of the Boundary Value Problem

Here, we have considered the three-dimensional power-law nano non-Newtonian fluid model. The flow is incompressible, steady, laminar over a linearly stretching sheet with the velocity $u_w = ax$ and $v_w = by$ in X and Y-direction respectively. Here, the stretched sheet is exposed to a homogeneous magnetic field B that is directed in the surface's normal direction. The conditions of convective boundaries are considered for the flow analysis. Heat generation/absorption impacts, as well as the impact of thermal radiation, are also considered in the heat transfer study.

We have taken the following parameters for the flow analysis.

$T_\infty$ - Temperature at Infinite distance from the sheet's surface

$C_\infty$ - Concentration at Infinite distance from the sheet's surface

$h_f$ - Heat transfer coefficient

$h_s$ - Convective mass transfer coefficient

Convective heat transfer mode is used to heat or cool the sheet's surface by maintaining a hot fluid temperature $T_f$ and a convective concentration of fluid $C_f$.

We have used the following boundary value flow governing equations.

$$\frac{\partial u}{\partial x} + \frac{\partial v}{\partial y} + \frac{\partial w}{\partial z} = 0 \tag{1}$$

$$u\frac{\partial u}{\partial x}+v\frac{\partial u}{\partial y}+w\frac{\partial u}{\partial z}=-\frac{\lambda}{\rho}\frac{\partial}{\partial z}\left(-\frac{\partial u}{\partial z}\right)^{n}-\frac{\sigma B^{2}}{\rho}u \tag{2}$$

$$u\frac{\partial v}{\partial x}+v\frac{\partial v}{\partial y}+w\frac{\partial v}{\partial z}=-\frac{\lambda}{\rho}\frac{\partial}{\partial z}\left[\left(-\frac{\partial u}{\partial z}\right)^{n-1}\frac{\partial v}{\partial z}\right]-\frac{\sigma B^{2}}{\rho}v \tag{3}$$

$$u\frac{\partial T}{\partial x}+v\frac{\partial T}{\partial y}+w\frac{\partial T}{\partial z}=\alpha\frac{\partial^{2}T}{\partial z^{2}}+\tau\left[D_{B}\left(\frac{\partial T}{\partial z}\frac{\partial C}{\partial z}\right)+\frac{D_{T}}{T_{\infty}}\left(\frac{\partial T}{\partial z}\right)^{2}\right]+\frac{Q_{0}}{\rho c_{p}}(T-T_{\infty})-\frac{1}{\rho c_{p}}\frac{\partial q_{r}}{\partial z} \tag{4}$$

$$u\frac{\partial C}{\partial x}+v\frac{\partial C}{\partial y}+w\frac{\partial C}{\partial z}=D_{B}\left(\frac{\partial^{2}C}{\partial z^{2}}\right)+\frac{D_{T}}{T_{\infty}}\frac{\partial^{2}T}{\partial z^{2}} \tag{5}$$

Boundary values for convective mode are given by

$$u=u_{w}=ax,\ v=v_{w}=by,\ w=0,-k\frac{\partial T}{\partial z}=h_{f}(T_{f}-T),-D_{B}\frac{\partial C}{\partial z}=h_{s}(C_{f}-C)$$
$$\text{at } z=0,u=0,v=0,w=0,T=T_{\infty},C=C_{\infty} \text{ at } z=\infty \tag{6}$$

Where,

$u$ - Velocity in the $x$ direction, $v$ -Velocity in the $y$ direction, $w$ -Velocity in the $z$ direction

$T$ - Fluid temperature, $C$ -Fluid concentration, $\rho$-Fluid density, $\tau$-Heat capacitance ratio

$D_T$ - Thermophoresis diffusion coefficient, $D_B$ -Brownian diffusion coefficient, $n$ : flow index

$\lambda$ (> 0) - Rheological constant, $\sigma$-electrical conductivity of the fluid, $\alpha$-thermal diffusivity

$Q_0$ : coefficient of internal heat generation, $q_r$ -radiative heat flux.

$q_r$ is defined as $q_r = \dfrac{-4\sigma^* {T_\infty}^3}{3k^*} \dfrac{\partial T^4}{\partial z}$

Where $\sigma^*$ - the Stefan-Boltzmann constant, $k^*$ - absorption coefficient.

Now, expanding $T^4$ about $T_\infty$ and neglecting higher terms, we get following expression:

$$T^4 = {T_\infty}^4 + 4{T_\infty}^3 T - 4{T_\infty}^3 T_\infty$$

$$\frac{\partial q_r}{\partial z} = \frac{\partial}{\partial z}\left(\frac{-4\sigma^* {T_\infty}^3}{3k^*} \frac{\partial T^4}{\partial z}\right)$$

$$\frac{\partial q_r}{\partial z} = \frac{-16\sigma^* {T_\infty}^3}{3k^*} \frac{\partial^2 T}{\partial z^2} \tag{7}$$

By putting $\dfrac{\partial q_r}{\partial z}$ in equation (4), we get the following equation.

$$u\frac{\partial T}{\partial x} + v\frac{\partial T}{\partial y} + w\frac{\partial T}{\partial z} = \alpha \frac{\partial^2 T}{\partial z^2} + \tau\left[DB\left(\frac{\partial T}{\partial z}\frac{\partial C}{\partial z}\right) + \left(\frac{D_T}{T_\infty}\frac{\partial T}{\partial z}\right)^2\right]$$

$$+\frac{Q_0}{\rho c_p}(T - T_\infty) + \frac{1}{\rho c_p}\frac{-16\sigma^* {T_\infty}^3}{3k^*}\frac{\partial^2 T}{\partial z^2} \tag{8}$$

## 3. Invariance Analysis by Generalized Group Theoretic Method

We have used the following dependent and independent absolute invariants to convert governing partial differential equations into ordinary differential equations invariantly. (Shukla *et al*. 2020)

$$\begin{cases} \eta = d_1 z(x)^{\frac{1-n}{1+n}} \\ H_1(\eta) = \frac{u}{d_2 x} \\ H_2(\eta) = \frac{v}{d_3 y} \\ H_3(\eta) = \frac{W}{d_4(x)^{\frac{n-1}{1+n}}} \\ H_4(\eta) = \theta = \frac{T-T_\infty}{T_f-T_\infty} \\ H_5(\eta) = \phi = \frac{C-C_\infty}{C_f-C_\infty} \end{cases}$$

We have assumed the following values for the coefficients and parameters.

$$d^1 = \left(\frac{a^{2-n}}{\frac{\lambda}{\rho}}\right)^{\frac{1}{n+1}}, d_2 = a \quad d_3 = b, \quad d_4 = -a\left(\frac{a^{n-2}}{\frac{\rho}{\lambda}}\right)^{\frac{1}{n+1}}$$

$$pr = \frac{\rho c_p u_w x}{k}(Re)^{\frac{-2}{n+1}}, \quad Re = \frac{(u_w)^{2-n} x^n \rho}{\lambda}, \; M \; \frac{\sigma B^2}{\rho}$$

$$Bi_1 = \frac{h_f}{k} x(Re)^{\frac{-1}{n+1}}, \quad N_b = \tau D_B \frac{(C_f - C_\infty)}{\alpha}, \quad R_d = \frac{-16\sigma T_\infty^{\,3}}{3k^*}, \quad \lambda_1 = \frac{Q_0}{\rho\alpha c_p} \tag{10}$$

Where $Re$-local Reynolds number, $pr$-generalised Prandtl number, $Le$-the Lewis number, $N_b$-Brownian motion parameter, $N_t$-thermophoresis parameter $Bi_1$ and $Bi_2$-generalised Biot number. We have taken skin-friction coefficients $C_{fx}$ and $C_{fy}$ along the $x$- and $y$-axes, the Nusselt number, and the Sherwood number for analysing the fluid flow. We have used the following equations for above parameters:

$$(Re)^{\frac{1}{n+1}} C_{fx} = -(H_1'(0))^n \tag{11}$$

$$(Re)^{\frac{1}{n+1}} C_{fy} = -\frac{a v_w}{b u_w}(H_1'(0))^{n-1} H_2'(0) \tag{12}$$

$$(Re)^{\frac{1}{n+1}} Nu_x = -(1 + R_d) H_4'(0) \tag{13}$$

$$(Re)^{\frac{1}{n+1}} Sh_x = -H_5'(0) \tag{14}$$

Differentiating absolute invariants of equation (9) with respect to similarity independent variable $\eta$ and applying on governing equations (1 to 5, 8), we obtain following equations.

$$aH_1 + bH_2 - aH_3^1 + \frac{1-n}{1+n} a\eta H_1' = 0 \tag{15}$$

$$a(H_1)^2 - aH_1'H_3 + \frac{1-n}{1+n} a\eta H_1'H_1 - na(-H_1')^{n-1} H_1'' + MH_1 = 0 \tag{16}$$

$$b(H_1)^2 - aH_2'H_3 + \frac{1-n}{1+n} a\eta H_2'H_1 + a(n-1)(-H_1')^{n-2} H_2'H_1''' - a(-H_1')^{n-1} H_2'' + MH_2 = 0 \tag{17}$$

$$prH_4'H_3 - pr\frac{1-n}{1+n} \eta H_1H_4' + H_4'' - R_dH_4'' + \lambda_1 H_4 + N_bH_4'H_5' + N_t(H_4')^2 = 0 \tag{18}$$

$$H_5'' + \frac{N_t}{N_b} H_4'' + prLeH_5'H_3' - prLe\frac{1-n}{1+n} \eta H_1H_5' = 0 \tag{19}$$

Similarly, we have obtained the following equations of boundary conditions from equation (6).

$$At\,\eta = 0,\ H_1 = 1,\ H_2 = 1,\ H_3 = 0,\ H_4' = -Bi_1(1 - H_4),\ H_5' = -Bi_2(1 - H_5),$$
$$At\,\eta = \infty,\ H_1 = H_2 = H_3 = H_4 = H_5 = 0. \tag{20}$$

The following equations are obtained from equations (15-19)

$$H_1 = \mathcal{G}'_1, H_2 = \mathcal{G}'_2, H_3 = \tfrac{2n}{1+n} \mathcal{G}_1 + \tfrac{b}{a} \mathcal{G}_2 + \tfrac{1-n}{1+n} \eta \mathcal{G}'_1 \tag{21}$$

$$a(\mathcal{G}'_1)^2 - b\mathcal{G}''_1\ \mathcal{G}_2 - \tfrac{2n}{1+n}\, a\mathcal{G}''_1\mathcal{G}_1 - na(-\mathcal{G}''_1)^{n-1}\mathcal{G}'''_1 + M\mathcal{G}'_1 = 0, \tag{22}$$

$$b(\mathcal{G}'_2)^2 - b\mathcal{G}''_2\ \mathcal{G}_2 - \tfrac{2n}{1+n}\, a\mathcal{G}''_2\mathcal{G}_1 - a(n-1)(-\mathcal{G}''_1)^{n-2}\mathcal{G}''_2\mathcal{G}'''_1 - a(-\mathcal{G}''_1)^{n-1}\mathcal{G}'''_2 + M\mathcal{G}_2 = 0, \tag{23}$$

$$H''_4 + N_b H'_4 H'_5 + N_t (H'_4)^2 + \frac{b}{a}\, pr H'_4\, \mathcal{G}_2 + \frac{2n}{1+n}\, pr\, \mathcal{G}_1(\eta) H'_4 - R_a H'_4 + \lambda_1 H_4 \tag{24}$$

$$H''_5 + \frac{N_t}{N_b}\, H''_4 + \frac{b}{a}\, Le\, pr\, H'_5\, \mathcal{G}_2 + \frac{2n}{1+n}\, pr\, Le\, \mathcal{G}_1 H'_5 = 0 \tag{25}$$

## 4. Numerical Solution

We have transformed the aforementioned system of equations into a system of first order differential equations in order to use Bvp4c - MATLAB software.

By replacing functions $\mathcal{G}_1, \mathcal{G}'_1, \mathcal{G}''_1, \mathcal{G}_2, \mathcal{G}'_2, \mathcal{G}''_2, H_4, H'_4, H_5, H'_5$ by $y_i$, for $i = 1, 2, \ldots, 10$ respectively, we get the following equations.

$$y'_1 = y_2 \tag{26}$$

$$y'_2 = y_3 \tag{27}$$

$$y'_3 = \frac{(a(y_2)^2 - by_3y_4 - \tfrac{2n}{1+n}\, ay_1y_3 + My_2)}{na(-y_3)^{n-1}} \tag{28}$$

$$y'_4 = y_5 \tag{29}$$

$$y'_5 = y_6 \tag{30}$$

$$y'_6 = \frac{b(y_5)^2 - by_4y_6 - \tfrac{2n}{1+n}\, ay_1y_6 - a(n-1)(-y_3)^{n-2}y'_3y_6 + My_5}{a(-y_3)^{n-1}} \tag{31}$$

$$y'_7 = y_8 \tag{32}$$

$$y'_8 = \frac{-N_b y_8 y_{10} - N_t (y_8)^2 - \frac{b}{a} pr y_4 y_8 - \frac{2n}{1+n} pr y_1 y_8 - \lambda y_7}{1 - R_d} \tag{33}$$

$$y'_9 = y_{10} \tag{34}$$

$$y'_{10} = -\frac{N_t}{N_b} y'_8 - \frac{b}{a} Lepr y_4 y_{10} - \frac{2n}{1+n} prLe y_1 y_{10} \tag{35}$$

$$\eta = 0 \Rightarrow y_1 = y_4 = 0, y_2 = y_5 = 1$$

$$y_8 = -Bi_1(1 - y_7(0)), y_{10} = -Bi_2(1 - y_9(0))$$

$$\eta = \infty \Rightarrow y_1 = 0, y_4 = 0, y_7 = 0, y_9 = 0 \tag{36}$$

We have obtained the following equations from equations (11-14)

$$(Re)^{\frac{1}{n+1}} C_{fx} = -(H_1'(0))^n = -(\mathcal{G}_1''(0))^n = -(y_3(0))n \tag{37}$$

$$(Re)^{\frac{1}{n+1}} C_{fy} = -\frac{av_w}{bu_w}(H_1'(0))^{n-1} H_2'(0) = -\frac{av_w}{bu_w}(\mathcal{G}_1''(0))^{n-1} \mathcal{G}_2''(0)$$

$$\frac{u_w}{v_w}(Re)^{\frac{1}{n+1}} C_{fy} = -\frac{a}{b}(y_3(0))^{n-1} y_6(0) \tag{38}$$

$$(Re)^{-\frac{1}{n+1}} Nu_x = -(1 + R_d) H_4'(0) = -(1 + R_d) y_8(0) \tag{39}$$

$$(Re)^{-\frac{1}{n+1}} Sh_x = -H_5'(0) = -y_{10}(0) \tag{40}$$

## 6. Results and Discussion

We have used MATLAB bvp4c solver for analysing fluid flow problem. Tables 1 and 2 show the values for Skin friction coefficients, Nusselt number, and Sherwood number.

Table 1: Skin friction coefficient values for various parameters in the $x$ and $y$ directions

| $n$ | $a$ | $b$ | $pr$ | $N_t$ | $N_b$ | $M$ | $R_d$ | $Le$ | $\lambda$ | $Cf_x$ | $Cf_y$ |
|---|---|---|---|---|---|---|---|---|---|---|---|
| 1 | 1 | 1 | 1 | 0.1 | 0.1 | 0.5 | 0 | 0.2 | 0 | 1.7538893508 | 1.7538893508 |
| 1 | 1 | 1 | 1 | 0.2 | 0.1 | 0.5 | 0 | 0.2 | 0 | 1.7538897120 | 1.7538897120 |
| 1 | 1 | 1 | 1 | 0.3 | 0.1 | 0.5 | 0 | 0.2 | 0 | 1.7538902961 | 1.7538902961 |
| 1 | 1 | 1 | 1 | 0.1 | 0.1 | 0.5 | 0 | 0.2 | 0 | 1.7538893508 | 1.7538893508 |
| 1 | 1 | 1 | 1 | 0.1 | 0.2 | 0.5 | 0 | 0.2 | 0 | 1.7538895038 | 1.7538895038 |
| 1 | 1 | 1 | 1 | 0.1 | 0.3 | 0.5 | 0 | 0.2 | 0 | 1.7538896175 | 1.7538896175 |
| 1 | 1 | 1 | 1 | 0.1 | 0.1 | 0.5 | 0 | 0.2 | 0 | 1.7538893508 | 1.7538893508 |
| 1 | 1 | 1 | 1 | 0.1 | 0.1 | 1.2 | 0 | 0.2 | 0 | 1.9058126194 | 1.9058126194 |
| 1 | 1 | 1 | 1 | 0.1 | 0.1 | 1.5 | 0 | 0.2 | 0 | 1.9704591416 | 1.9704591416 |
| 1 | 1 | 1 | 1 | 0.1 | 0.1 | 0.5 | 0 | 0.2 | 0.2 | 1.7538900002 | 1.7538900002 |
| 1 | 1 | 1 | 1 | 0.1 | 0.1 | 0.5 | 0.1 | 0.2 | 0.2 | 1.7538901651 | 1.7538901651 |
| 1 | 1 | 1 | 1 | 0.1 | 0.1 | 0.5 | 0.2 | 0.2 | 0.2 | 1.7538907395 | 1.7538907395 |
| 1 | 1 | 1 | 1 | 0.1 | 0.1 | 0.5 | 0 | 0 | 0.2 | 1.7538899995 | 1.7538899995 |
| 1 | 1 | 1 | 1 | 0.1 | 0.1 | 0.5 | 0 | 0.1 | 0.2 | 1.7538899984 | 1.7538899984 |
| 1 | 1 | 1 | 1 | 0.1 | 0.1 | 0.5 | 0 | 0.2 | 0.2 | 1.7538900002 | 1.7538900002 |
| 1 | 10 | 2 | 2 | 0.1 | 0.1 | 0.5 | 0.1 | 0.2 | 0.2 | 1.5511878626 | 1.8971685570 |
| 1 | 10 | 4 | 2 | 0.1 | 0.1 | 0.5 | 0.1 | 0.2 | 0.2 | 2.8042554030 | 1.3992670114 |
| 1 | 10 | 6 | 2 | 0.1 | 0.1 | 0.5 | 0.1 | 0.2 | 0.2 | 3.1138892553 | 1.1463275550 |

From Table 1, it is observed that the value of skin friction coefficient in $X$ and $Y$ direction both enhances with rising values of the thermophoresis parameter $N_t$ as well as thermal radiation $R_d$. The reason behind it is that if the thermophoresis parameter is increasing the temperature and concentration, differences between the surface of the semi-infinite vertical plate and the ambient fluid are increasing and hence accelerates the heat transfer rate. Table 1 shows the skin friction coefficient for various values of the Brownian motion parameter $N_b$.

The skin friction coefficient in both directions is seen to grow with increasing values of the Brownian motion parameter $N_b$ and opposite behaviour observed for Lewis number $Le$. The skin friction coefficient increases as the magnetic field parameter $M$ increases because it reflects an increase in surface velocity gradients. A similar phenomenon is noticed in Table 1. Effect of stretching ratio parameter significantly affects skin friction coefficient. An increase in parameter $b$, the skin friction coefficient in the $X$ direction rises, whereas the $Y$ direction exhibits the opposite behaviour.

Table 2: Sherwood number and Nusselt number Values for different parameters

| $n$ | $b$ | $n$ | $N_t$ | $N_b$ | $M$ | $pr$ | $Le$ | $\lambda$ | $Rd$ | $Sh_x$ | $Nu_x$ |
|---|---|---|---|---|---|---|---|---|---|---|---|
| 1 | 1 | 1 | 0.1 | 0.1 | 0.5 | 1 | 0.2 | 0 | 0 | 0.1055262378 | 0.3824750511 |
| 1 | 1 | 1 | 0.2 | 0.1 | 0.5 | 1 | 0.2 | 0 | 0 | -0.0451858252 | 0.3801468924 |
| 1 | 1 | 1 | 0.3 | 0.1 | 0.5 | 1 | 0.2 | 0 | 0 | -0.1918276471 | 0.3777829817 |
| 1 | 1 | 1 | 0.1 | 0.1 | 0.5 | 1 | 0.2 | 0 | 0 | 0.1055262378 | 0.3824750511 |
| 1 | 1 | 1 | 0.1 | 0.2 | 0.5 | 1 | 0.2 | 0 | 0 | 0.1838693036 | 0.3801079022 |
| 1 | 1 | 1 | 0.1 | 0.3 | 0.5 | 1 | 0.2 | 0 | 0 | 0.2099947839 | 0.3777045682 |
| 1 | 1 | 1 | 0.1 | 0.1 | 0.5 | 1 | 0.2 | 0 | 0 | 0.1055262378 | 0.3824750511 |
| 1 | 1 | 1 | 0.1 | 0.1 | 1.2 | 1 | 0.2 | 0 | 0 | 0.1066120068 | 0.3811253420 |
| 1 | 1 | 1 | 0.1 | 0.1 | 1.5 | 1 | 0.2 | 0 | 0 | 0.1070520017 | 0.3803950922 |
| 1 | 1 | 1 | 0.1 | 0.1 | 0.5 | 0.7 | 0.2 | 0 | 0 | 0.6808097648 | -0.0591201311 |
| 1 | 1 | 1 | 0.1 | 0.1 | 0.5 | 1.2 | 0.2 | 0 | 0 | 0.4517559332 | 0.0767238041 |
| 1 | 1 | 1 | 0.1 | 0.1 | 0.5 | 1.7 | 0.2 | 0 | 0 | 0.1075016163 | 0.4341594390 |
| 1 | 1 | 1 | 0.1 | 0.1 | 0.5 | 1 | 0 | 0.2 | 0 | 0.0640340920 | 0.3645373365 |
| 1 | 1 | 1 | 0.1 | 0.1 | 0.5 | 1 | 0.1 | 0.2 | 0 | 0.0926736299 | 0.3644023170 |
| 1 | 1 | 1 | 0.1 | 0.1 | 0.5 | 1 | 0.2 | 0 | 0 | 0.1055262378 | 0.3824750511 |
| 1 | 1 | 1 | 0.1 | 0.1 | 0.5 | 1 | 0.2 | 0.2 | 0 | 0.1210982576 | 0.3642872395 |
| 1 | 1 | 1 | 0.1 | 0.1 | 0.5 | 2 | 0.2 | 0.2 | 0.1 | 0.1154854564 | 0.4960100946 |
| 1 | 1 | 1.2 | 0.1 | 0.1 | 0.5 | 2 | 0.2 | 0.2 | 0.1 | 0.1151724519 | 0.4966261688 |
| 1 | 1 | 1.3 | 0.1 | 0.1 | 0.5 | 2 | 0.2 | 0.2 | 0.1 | 0.1150959844 | 0.4968748668 |
| 1 | 1 | 1.4 | 0.1 | 0.1 | 0.5 | 2 | 0.2 | 0.2 | 0.1 | 0.1150477775 | 0.4970963117 |

Table 2 indicates the effect of various parameters on the Sherwood number and Nusselt number. Growing thermophoresis parameter values are accompanied by decreasing Sharwood and Nusselt numbers. Table 2 demonstrates that when the Brownian motion parameter increases, the rate of heat transmission slows down, resulting in a fall in the Nusselt number and an observed increase in the Sherwood number. It is observed that the Nusselt number decreases and the Sherwood number increases with an acceleration of the magnetic parameter .

The Lorentz force is increased when the magnetic parameter increases, slowing down fluid motion and lowering the rate of heat flux in the process. By increasing the value of the Lewis number, nanoparticle volume fraction distribution decreases, because of reduction in mass diffusion. This, in turn, increases the Sherwood number, with the opposite effect being seen on the Nusselt number. Based on the table's numerical values, it can be determined that as the radiation parameter is raised, the Sherwood number falls and the Nusselt number rises. An analogous result was noted with the Prandtl number. The Sherwood number rises, the heat generation parameter lambda increases, and the Nusselt number decreases. The Sherwood number decreases as $n$ (the power-law index) increases, but the Nusselt number increases.

Figures 1 and 2 depict, how the Lewis number changes the Nusselt and Sherwood numbers in response to thermophoresis and thermal radiation, respectively. The Nusselt number decreases as the thermophoresis parameter and Lewis number grow, while inverse patterns are seen as the thermal radiation parameter increases. As thermophoresis and Lewis numbers rise, Sherwood number tends to increase; conversely, as the thermal radiation parameter increases, it tends to decrease.

Figures 3 and 4 show the impact of the heat source/sink parameter under the influence of thermal radiation and thermophoresis parameter on the Nusselt number and Sherwood number. Figures 5 and 6 demonstrate the influence of the Brownian motion parameter, the thermophoresis parameter, and the thermal radiation parameter on the Sherwood number and Nusselt number respectively. Sherwood number decreases as thermal radiation parameter value increases. Nusselt number increasing as a result of the thermal radiation parameter increasing.

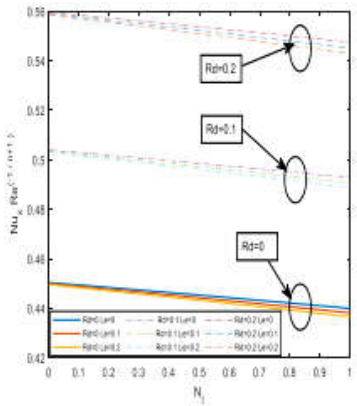



*Figure 1 Impact of thermal radiation and thermophoresis on the Nusselt number under the impact of Lewis number*

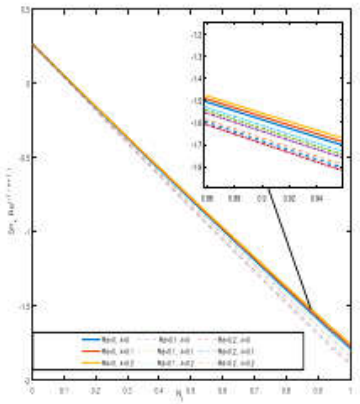


***Figure 2 Influence of Lewis number on the Sherwood number under the impact of thermophoresis and thermal radiation***

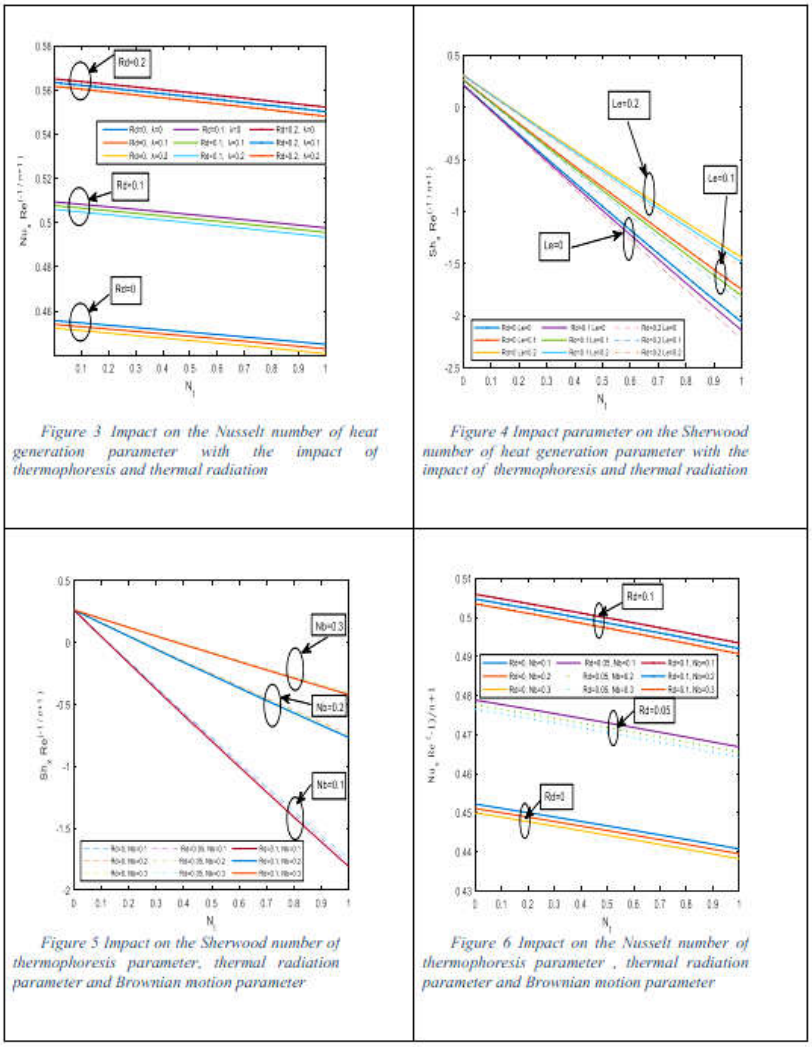



*Figure 3 Impact on the Nusselt number of heat generation parameter with the impact of thermophoresis and thermal radiation*

*Figure 4 Impact parameter on the Sherwood number of heat generation parameter with the impact of thermophoresis and thermal radiation*

*Figure 5 Impact on the Sherwood number of thermophoresis parameter, thermal radiation parameter and Brownian motion parameter*

*Figure 6 Impact on the Nusselt number of thermophoresis parameter , thermal radiation parameter and Brownian motion parameter*

## 5. Conclusion

We have used both similarity dependent and independent invariants to get a similarity solution for the boundary value problem associated with power-law nanofluid flow. The power-law nanofluid problem's governing equations have been converted into ordinary differential equations with the help of invariants. The numerical solutions of derived ordinary differential equations are utilized by using MATLAB bvp4c software to find the effects of various parameters like Nusselt number, Sharwood number and Skin friction coefficients on fluid flow. The following are the findings of the analysis of the fluid flow using invariants.

- The findings indicate that an increase in the Lewis number $Le$ results in a drop in the coefficient of skin friction in the $x$ and $y$ directions, an increase in the Sharwood number, and a decrease in the Nusselt number.
- An increase in the magnetic parameter $M$ causes the skin friction coefficient to increase in both the $x$ and $y$ directions, the Nusselt number decreases, and the Sharwood number increases.
- A rise in the power-law index , a fall in the Sherwood number, and an increase in the Nusselt number.
- The Sherwood and Nusselt numbers decrease with an increase in the thermophoresis parameter.
- As the radiation parameter increases, the Nusselt number rises while the Sherwood number reduces.

**Conflict of Interest Statement**

We (authors) do not have any conflict of interest (financial or academic) for this work.

## REFERENCES

Abdul, S., Yufeng N., Zahir, S., Abdullah, D., Waris, K. and Saeed, I. (2018): Three-Dimensional Nanofluid Flow with Heat and Mass Transfer Analysis over a Linear Stretching Surface with Convective Boundary Conditions, *Applied Sciences*, Vol. 8, pp. 1-18.

Ahmed, S. E., Ramadan, A. M., Abd Elraheem, M. A. and Mahmoud, S. S. (2019): Magnetohydrodynamic Maxwell Nanofluids Flow over a Stretching Surface through a Porous Medium: Effects of Non-Linear Thermal Radiation, Convective Boundary Conditions and Heat Generation/Absorption, *International Journal of Aerospace and Mechanical Engineering* (World Academy of Science, Engineering and Technology), Vol. 13, pp. 436-443.

Aisha, A., Mir, N. A., Farooq, M., Javed, M., Ahmad, S., Malik, M. Y. and Alshomrani, A. S, (2018): Physical aspects of heat generation/absorption in the second-grade fluid flow due to Riga plate: Application of Cattaneo-Christov approach, *Results in Physics*, Vol. 9, pp. 955-960.

Animasaun, I. L., Adebile, E. A. and Fagbade, A. I. (2016): Casson fluid flow with variable thermo-physical property along exponentially stretching sheet with suction and exponentially decaying internal heat generation using the homotopy analysis method, *Journal of the Nigerian Mathematical Society*, Vol. 35, pp. 1-17.

Awais, M., Hayat, T., Irum S. and Alsaedi, A., (2015): Heat Generation/Absorption Effects in a Boundary Layer Stretched Flow of Maxwell Nanofluid: Analytic and Numeric Solutions, PLOS ONE, Vol. 10, No. 6. Bilal, M., Sagheer, M. and Hussain, S. (September 2018), Maxwell nanofluid flow with nonlinear radiative heat flux, *Alexandria Engineering Journal*, Vol. 57(3), pp. 1917-1925.

Chuo-Jeng, H. and Kuo-Ann, Y. (2021): Nonlinear Radiation and Variable Viscosity Effects on Free Convection of a Power-Law Nanofluid Over a Truncated Cone in Porous Media with Zero Nanoparticles Flux and Internal Heat Generation, *Journal of Thermal Science and Engineering Applications*, Vol. 13.

Dianchen, L., Ramzan, M., Huda, N., Jae, D. C., and Umer, F. (2018): Nonlinear radiation efect on MHD Carreau nanofuid fow over a radially stretching surface with zero mass fux at the surface, *Scientific Reports*, Vol. 8, p. 3709.

Feroz, A. S., Rizwan, U. H., Qasem, M. and Qiang, Z. (March 2018): Heat generation/absorption and nonlinear radiation effects on stagnation point flow of nanofluid along a moving surface, *Results in Physics*, Vol. 8, pp. 404-414.

Ganesh, K., Ramesh, G. K. and Gireesha, B. J. (2018): Thermal analysis of generalized Burgers nanofluid over a stretching sheet with nonlinear radiation and non-uniform heat source/sink, *Archives of Thermodynamics*, Vol. 39(2), pp. 97-122.

Kalpna, S. and Sumit, Gupta (2017): Viscous Dissipation and Thermal Radiation effects in MHD flow of Jeffrey Nanofluid through Impermeable Surface with Heat Generation/Absorption, *Nonlinear Engineering*, Vol. 6(2), pp. 153-166.

Hasmawani, H., Muhammad, K. A., Nazila I., Norhafizah, M. S., and Mohd, Z. S. (2019): Thermal Radiation Effect on MHD Stagnation Point flow of Williamson Fluid over a stretching Surface, Results in Physics, Conference Series 1366(2019) 012011, 2nd International Conference on Applied & Industrial Mathematics and Statistics 23-25 July 2019, Kuantan, Pahang, Malaysia: IOP

Hayat, T., Qayyum, S., Shehzad, S. A. and Alsaedi, A. (2017): Simultaneous effects of heat generation/absorption and thermal radiation in magnetohydrodynamics (MHD) flow of Maxwell nanofluid towards a stretched surface, *Results in Physics*, Vol. 7, pp. 562-573.

Hiranmoy, M., Mohammed, A. and Precious S., (2019): Dual solutions for three- dimensional magnetohydrodynamic nanofluid flow with entropy generation, *Journal of Computational Design and Engineering*, Vol. 6(4), pp. 657-665.

Kalidas, D., Tanmoy, C. and Prabir, K. K. (September 2018): Effect of magnetic field on Oldroyd-B type nanofluid flow over a permeable stretching surface, *Propulsion and Power Research*, Vol. 7(3), pp. 238-246.

Khan, W. A., Masood, K., and Malik, R. (2014): Three-Dimensional Flow of an Oldroyd-B Nanofluid towards Stretching Surface with Heat Generation/Absorption, *PLOS ONE*, Vol. 9(8).

Lalrinpuia, T. and Surender, O. (2019): Entropy generation in MHD nanofuid fow with heat source/sink, *SN Applied Sciences*, Vol. 1, No. 1672.

Mabood, F., Bognár, G. and Shafiq, A. (2020): Impact of heat generation/absorption of magnetohydrodynamics Oldroyd-B fluid impinging on an inclined stretching sheet with radiation, *Sci Rep*., Vol. 10.

Makinde (2011): Similarity Solution for Natural Convection from A Moving Vertical Plate with Internal Heat Generation and A Convective Boundary Condition, *Thermal Science*, Vol. 15(1), pp. 137-143.

Patel, M., Patel, J., and Timol, M. G., (2015): Laminar Boundary Layer Flow of Sisko Fluid, *Applications and Applied Mathematics*, (AAM), Vol. 10(2), pp. 909-918.

Pandey, A. K. and Manoj, K. (2018): Effects Of Viscous Dissipation and Heat Generation/Absorption on Nanofluid Flow Over An Unsteady Stretching Surface With Thermal Radiation And Thermophoresis, *Nanoscience and Technology An International Journal*, Vol. 9(4), pp. 325-341.

Sulochana, C., Ashwinkumar, G. P., and Sandeep, N. (2016): Similarity solution of 3D Casson nanofluid flow over a stretching sheet with convective boundary conditions, *Journal of the Nigerian Mathematical Society*, Vol. 35(1), pp. 128-141.

SUS., Choi. (1995): Enhancing thermal conductivity of fluids with nanoparticles, developments and applications of non-Newtonian flows, *ASME FED 231/MD* Vol. 66, pp. 99-105.

Tesfaye, K., Eshetu, H., Gurju, A. and Tadesse, W. (2020): Heat and Mass Transfer in Unsteady Boundary Layer Flow of Williamson Nanofluids, *Journal of Applied Mathematics*, Vol. 2020, 13 pages.

Thiagarajan, M. and Dinesh, M. (2019): Effects of thermal radiation and heat generation on hydromagnetic flow of nanofluid over an exponentially stretching sheet in a porous medium with viscous dissipation, *World Scientific News*, Vol. 128(2), pp. 130-147.

Umadevi, P. and Nithyadevi, N. (2016): Magneto-convection of water-based nanofluids inside an enclosure having uniform heat generation and various thermal boundaries, *Journal of the Nigerian Mathematical Society*, Vol. 35(1), pp. 82-92.

Waqas, M., Ijaz Khan, M., Hayat, T. and Alsaedi, A. (2017): Stratified flow of an Oldroyd-B nanoliquid with heat generation, *Results in Physics*, Vol. 7, pp. 2489-2496.

Shukla, H., Patel, J., Surati, H. C., Patel, M. and Timol, M. G. (2017): Similarity solution of forced convection flow of Powell-Eyring and Prandtl-Eyring fluids by group-theoretic method, *Mathematical Journal of Interdisciplinary Sciences*, Vol. 5(2), pp. 151- 165.

Shukla, H., Surati, H. C. and Timol, M. G. (2018): Similarity analysis of three dimensional nanofluid flow by deductive group theoretic method, *Applications and Applied Mathematics-An International Journal*, Vol. 13(2), pp. 1260-1272.

Shukla, H., Surati, H. C., and Timol, M. G. (2020): Similarity Analysis of MHD Three Dimensional Nanofluid Flow for Non-Newtonian Power-Law Model over Linearly Stretching Sheet with Convective Boundary Conditions, *International Journal of Heat and Technology*, Vol. 38(1), pp. 203-212.

1. Department of Mathematics,
Government Engineering College,
Gandhinagar-382028, GTU, India
E-mail: hsshukla94@gmail.com

(*Received*, September 25, 2024)
(*Revised*, December 23, 2024)

2. B. Tech Student,
IIIT, Vadodara, Gandhinagar-382028, India
E-mail: shivanshidave10@gmail.com

3. Department of Instrumental and Control Engineering,
Government Engineering College,
Gandhinagar-382028, GTU, India;
E-mail: kcdave@gecg28.ac.in

4. Department of Mathematics,,
Government Engineering College,
Gandhinagar-382028, GTU, India
E-mail: ashwin.rathodmaths@gmail.com

5. Department of Mathematics,
Government Engineering College,
Gandhinagar-382028, GTU, India
E-mail: nirmaths@gmail.com

6. Department of Electrical, Engineering
Government Engineering College,
Gandhinagar-382028, GTU, India
E-mail: jignashaprajapati@gecg28.ac.in